HTML ABSTRACT + LINKS

GaN metal-oxide-semiconductor high-electron-mobility-transistor with atomic layer deposited Al_2O_3 as gate dielectric

P. D. Ye,[a] B. Yang, K. K. Ng, and J. Bude
Agere Systems, 555 Union Boulevard, Allentown, Pennsylvania 18109

G. D. Wilk
ASM America, 3440 East University Drive, Phoenix, Arizona 85034

S. Halder and J. C. M. Hwang
Lehigh University, 5 East Packer Avenue, Bethlehem, Pennsylvania 18015

(Received 19 July 2004; accepted 17 December 2004; published online 31 January 2005)

We report on a GaN metal-oxide-semiconductor high-electron-mobility-transistor (MOS-HEMT) using atomic-layer-deposited (ALD) Al_2O_3 as the gate dielectric. Compared to a conventional GaN high-electron-mobility-transistor (HEMT) of similar design, the MOS-HEMT exhibits several orders of magnitude lower gate leakage and several times higher breakdown voltage and channel current. This implies that the ALD Al_2O_3/AlGaN interface is of high quality and the ALD Al_2O_3/AlGaN/GaN MOS-HEMT is of high potential for high-power rf applications. In addition, the high-quality ALD Al_2O_3 gate dielectric allows the effective two-dimensional (2D) electron mobility at the AlGaN/GaN heterojunction to be measured under a high transverse field. The resulting effective 2D electron mobility is much higher than that typical of Si, GaAs or InGaAs metal-oxide-semiconductor field-effect-transistors (MOSFETs). © *2005 American Institute of Physics*. [DOI: 10.1063/1.1861122]

One of the major factors that limit the performance and reliability of GaN high-electron-mobility-transistors (HEMTs) for high-power radio-frequency (rf) applications is their relatively high gate leakage. The gate leakage reduces the breakdown voltage and the power-added efficiency while increasing the noise figure. To help solve the problem, significant progress has been made on metal-insulator-semiconductor high-electron-mobility-transistors (MIS-HEMTs) and metal-oxide-semiconductor high-electron-mobility-transistors (MOS-HEMTs) using SiO_2,[1–5] Si_3N_4,[6,7] Al_2O_3[8,9] (formed by electron cyclotron resonance plasma oxidation of Al), and other oxides.[10] However these gate dielectrics and their associated processes may not be readily scalable for low-cost and high-yield manufacture. Atomic layer deposition (ALD) is a surface controlled layer-by-layer process for the deposition of thin films with atomic layer accuracy. Each atomic layer formed in the sequential process is a result of saturated surface controlled chemical reactions. The thickness control of the ALD films thus scalability is much superior than those of the plasma-enhanced-chemical-vapor-deposition (PECVD) grown SiO_2 and Si_3N_4. The quality of the ALD Al_2O_3 is also much higher than those deposited by other methods, i.e., sputtering and electron-beam deposition, in terms of uniformity, defect density and stoichiometric ratio of the films.

In this letter, we report on a GaN MOS-HEMT with atomic-layer-deposited Al_2O_3 as the gate dielectric. Similar to SiO_2, Si_3N_4, and Sc_2O_3,[10] Al_2O_3 can significantly reduce the gate leakage of GaN HEMTs. Al_2O_3 offers additional advantages of a large band gap (9 eV), high dielectric constant ($k \sim 10$), high breakdown field (10^7 V/cm), thermal stability (amorphous up to at least 1000 °C),[11] and chemical stability against AlGaN (without interdiffusion and interaction of Si and Al). Furthermore, ALD Al_2O_3 has become one of the leading candidates to replace SiO_2 in future-generation Si CMOS digital ICs.[12] The ALD equipment for Al_2O_3 has demonstrated low defect density, high uniformity, and nanometer scalability. The ALD Al_2O_3 process is *ex situ*, robust and highly manufacturable. We reported earlier excellent performance of GaAs and InGaAs MOSFETs with ALD Al_2O_3.[13–15] We now report similar performance advantages of an ALD Al_2O_3/AlGaN/GaN MOS-HEMT.

Figure 1 shows the cross sections of an ALD Al_2O_3/AlGaN/GaN MOS-HEMT and a conventional AlGaN/GaN HEMT of similar design. A 40 nm undoped AlN buffer layer, a 3 μm undoped GaN layer, and a 30 nm undoped $Al_{0.2}Ga_{0.8}N$ layer were sequentially grown by metal-organic chemical vapor deposition on a 2-in. sapphire substrate. After these layers were grown, the wafer was transferred via room ambient to an ASM Pulsar2000™ ALD module. A 16-nm-thick Al_2O_3 layer was deposited at 300 °C then followed by annealing at 600 °C per 60 s in oxygen ambient. Device isolation was achieved by nitrogen implanatation. Using a wet etch in diluted HF, the oxide on the source and drain regions was removed while the gate region was protected by photoresist. Ohmic contacts were formed by electron-beam deposition of Ti/Al/Ni/Au and a lift-off process, followed by

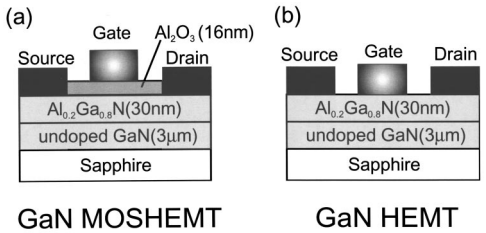

FIG. 1. Cross sections of (a) an ALD Al_2O_3/AlGaN/GaN MOS-HEMT and (b) a conventional AlGaN/GaN HEMT of similar design.

[a]Permanent address: School of Electrical and Computer Engineering, Purdue University, 465 Northwestern Avenue, West Lafayette, Indiana 47907-2035; electronic mail: yep@ecn.purdue.edu

 © 2005 American Institute of Physics
Downloaded 29 Oct 2006 to 128.46.221.220. Redistribution subject to AIP license or copyright, see http://apl.aip.org/apl/copyright.jsp

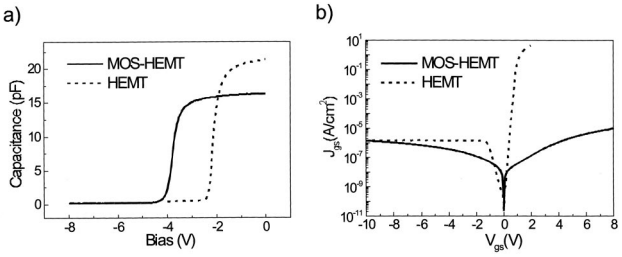

FIG. 2. Measured (a) *C–V* characteristics and (b) gate leakage of the MOS-HEMT (solid line) and the baseline HEMT (dashed line).

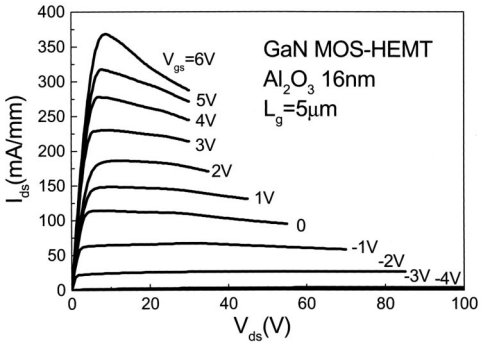

FIG. 3. Measured *I–V* characteristics of the MOS-HEMT. The negative output conductance under high gate biases ($V_{gs} \geqslant 0$) is due to self-heating.

an 850 °C anneal in a nitrogen ambient, which also activated the previously implanted nitrogen. Finally, Ni/Au metals were e-beam evaporated and lifted off to form the gate electrodes. All four levels of lithography (alignment, isolation, Ohmic, and gate) were done by using a contact aligner. The sheet resistance of the source/drain regions and their contact resistances were measured to be 700 Ω/sq. and 4.0 Ω mm, respectively. The gate lengths, L_g, of the measured devices are 0.65, 1, 5, and 10 μm. The gate width, W_g, is 100 μm. The relatively long gate length (i.e., 5 and 10 μm) is necessary for accurate characterization of the effective 2D electron mobility at the AlGaN/GaN heterojunction, in order to reduce the error in extracting the series resistance. The source-to-gate and the gate-to-drain spacings are 2 μm.

Figure 2(a) shows the *C–V* characteristics measured at 1 MHz on gate capacitors of both the MOS-HEMT and HEMT structures. Using a dielectric constant $\varepsilon_{\mathrm{AlGaN}}=8.8$ (Ref. 2) and a zero-bias capacitance $C_{\mathrm{HEMT}}=21$ pF, the AlGaN layer thickness of the HEMT is estimated to be 29 nm, which is within 3% of the design value of 30 nm. The Al_2O_3 thickness d_{OX} is estimated to be 10 nm by using the following equation:

$$\frac{1}{C_{\mathrm{MOS\text{-}HEMT}}}=\frac{1}{C_{\mathrm{OX}}}+\frac{1}{C_{\mathrm{HEMT}}}, \tag{1}$$

where $C_{\mathrm{MOS\text{-}HEMT}}=16$ pF is the zero-bias capacitance of the MOS-HEMT, $C_{\mathrm{OX}}=\varepsilon_0\cdot\varepsilon_{\mathrm{OX}}A/d_{\mathrm{OX}}$, ε_0 is vacuum permittivity, $\varepsilon_{\mathrm{OX}}=10$ is the dielectric constant of ALD Al_2O_3, and $A=8000\ \mu\mathrm{m}^2$ is the capacitor area. The estimated oxide thickness is significantly less than the design value of 16 nm, probably due to oxide compression by high temperature annealing or cleaning before the gate metal deposition. The transition from depletion to accumulation in the *C–V* characteristic of the MOS-HEMT is as sharp as that of the HEMT, which demonstrates the high-quality interface between Al_2O_3 and AlGaN. Figure 2(b) shows that the gate leakage of the MOS-HEMT is generally lower than that of the HEMT. Specifically, under a positive gate bias $V_{gs}=2$ V, the gate leakage current density of the MOS-HEMT is more than six orders of magnitude lower than that of the HEMT. The HEMT cannot be biased greater than 2 V. By contrast, the forward two-terminal breakdown voltage of the MOS-HEMTs is approximately 12 V. Using a breakdown field of 1.3 MV/cm across the 30 nm AlGaN layer, the breakdown field across the 16 nm Al_2O_3 layer is estimated to be greater than 5 MV/cm. This verifies the high quality of the ALD Al_2O_3.

Figure 3 shows that the *I–V* characteristics of the MOS-HEMT are well behaved over a drain bias V_{ds} of 0 to 100 V and a gate bias V_{gs} of −4 to 6 V. The pinch-off voltage is consistently −4 V. The maximum drain current density I_{ds}/W_g at $V_{gs}=6$ V is approximately 375 mA/mm. The off-state three-terminal breakdown voltage is approximately 145 V. The results indicate that ALD Al_2O_3 is an effective gate dielectric for AlGaN/GaN devices. Our devices have no widely observed abnormal *I–V* characteristics at positive gate biases, i.e., PECVD grown SiO_2 GaN MOS-HEMTs,[1] which are mostly related with the bulk traps in PECVD grown dielectrics or interface traps at insulating films on GaN.

Figures 4(a) and 4(b) illustrate the saturated ($V_{ds}=10$ V) drain current density and intrinsic transconductance g_m as a function of gate bias for both the MOS-HEMT and the HEMT. The drain current density of the HEMT is limited to 190 mA/mm at $V_{gs}=2$ V. By contrast, the drain current density of the MOS-HEMT is 450 mA/mm at $V_{gs}=8$ V and can be further increased under higher V_{gs}. The combination of higher breakdown voltage and higher drain current imply that the output power of the MOS-HEMT can be much higher that of the HEMT. Using $I_{ds}/W_g=e\cdot n_s\cdot v_{\mathrm{sat}}=450$ mA/mm and a saturated velocity $v_{\mathrm{sat}}=5\times10^6$ cm/s, the sheet carrier density n_s is estimated to be $6\times10^{12}/\mathrm{cm}^2$, which is within the range of values commonly observed for the heterojunction between undoped $Al_{0.2}Ga_{0.8}N$ and GaN. Figure 4(b) shows that the peak g_m is 100 and 120 mS/mm for the MOS-HEMT and the HEMT, respectively. The g_m was calculated from the measured extrinsic transconductance by accounting for the parasitic source resistance R_s of 5.4 and 5.9 Ω mm for the MOS-HEMT and the HEMT, respectively. The R_s values were measured on test structures fabricated alongside the MOS-HEMT and the HEMT according to the transmission line method (TLM). These g_m values are in agreement with theoretical estimates according to g_m

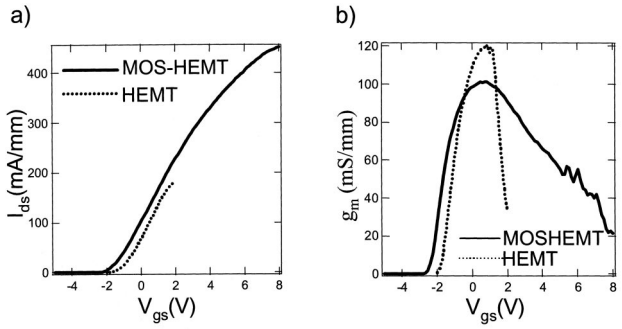

FIG. 4. Measured (a) transfer and (b) transconductance characteristics measured with the MOS-HEMT (solid line) and HEMT (dashed line) in saturation ($V_{ds}=10$ V).

Downloaded 29 Oct 2006 to 128.46.221.220. Redistribution subject to AIP license or copyright, see http://apl.aip.org/apl/copyright.jsp

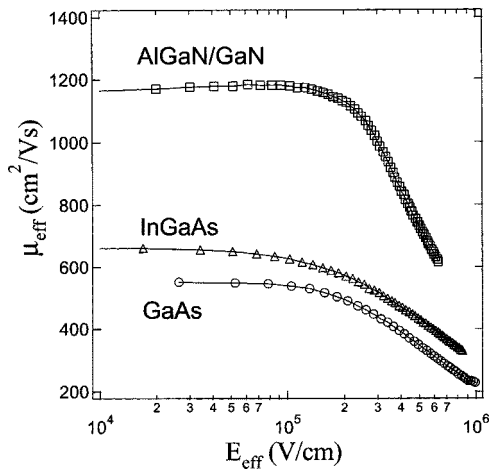

FIG. 5. Calculated effective 2D electron mobility vs. effective electric field at the AlGaN/GaN (squares), Al_2O_3/InGaAs (triangles), and Al_2O_3/GaAs (circles) interfaces.

$=v_{sat}\cdot C_{MOS\text{-}HEMT}$ or $g_m=v_{sat}\cdot C_{HEMT}$. Using $v_{sat}=5\times10^6$ cm/s, $C_{MOS\text{-}HEMT}=16$ pF, and $C_{HEMT}=21$ pF, g_m was estimated to be 102 and 133 mS/mm for the MOS-HEMT and the HEMT, respectively. The sheet resistances measured on TLM test structures are 700 and 950 Ω/ sq. for the MOS-HEMT and the HEMT, respectively.

The present AlGaN/GaN heterojunction is of such high quality that a strong accumulation current I_{acc} exists which allows I_{ds}/W_g to increase from 100 to 450 mA/mm when V_{gs} is increased from 0 to 8 V. This enables us to measure the effective 2D electron mobility μ_{eff} at the AlGaN/GaN heterojunction under high electron density and high transverse field for the first time. The 2D electron mobility is governed by Coulomb scattering and phonon scattering under low transverse field. It is dominated by interface roughness scattering and phonon scattering under strong accumulation. By measuring I_{ds} versus V_{gs} at $V_{ds}=0.1$ V, we extracted the intrinsic normalized channel resistance $R_{ch}=V_{ds}\cdot W_g/I_{acc}\cdot L_g$ with better than ±5% accuracy. The μ_{eff} can then be calculated according to

$$R_{ch}=\frac{1}{\mu_{eff}\cdot C_{MOS-HEMT}\cdot(V_{gs}-V_{Gi})} \tag{2}$$

where V_{Gi} is the zero-current intercept of V_{gs} extrapolated from the point of inflection of the I_{ds} versus V_{gs} characteristic.[16,17] Figure 5 plots μ_{eff} versus the effective electric field E_{eff}, with E_{eff} calculated according to

$$E_{eff}=\frac{V_{gs}-V_{Gi}}{2\varepsilon_{GaN}\cdot\left(\frac{d_{OX}}{\varepsilon_{OX}}+\frac{d_{AlGaN}}{\varepsilon_{AlGaN}}\right)}, \tag{3}$$

where the dielectric constants of GaN ε_{GaN} is taken to be 12.2 and the thickness of the AlGaN layer d_{AlGaN} is 30 nm. The resulted mobility of 1200 cm^2/V s under low transverse fields is consistent with the value obtained from the Hall measurement. The mobility of 640 cm^2/V s under a high transverse field of 0.6 MV/cm is much higher than 400 cm^2/V s, the universal mobility of Si MOSFETs under the same field.[18] It is also higher than the surface mobility of GaAs or InGaAs MOSFETs we observed earlier.[15] Such an improvement can be attributed to the higher quality of the AlGaN/GaN semiconductor–semiconductor interface than that of the oxide–semiconductor interfaces.[13] The *C–V* measurement and the frequency dispersion of transconductance measurement indicate that the midgap interface trap density of this material system is at the range of 10^{11}–10^{12}/cm^2 eV. The high quality of interfaces or the low interface trap densities are further verified by the excellent ac characteristics of GaN MOS-HEMTs, i.e., the small signal rf performance, the load-pull rf power measurements, and the pulsed drain characteristics of the devices.[19]

In summary, ALD Al_2O_3 was proven to be an excellent gate dielectric for GaN MOS-HEMTs. The present MOS-HEMT exhibits favorable characteristics when compared to GaN HEMTs. The present MOS-HEMT shows low leakage current, high breakdown voltage, strong accumulation, and high effective 2D electron mobility under both low and high transverse fields. These characteristics imply excellent potential of the ALD Al_2O_3/AlGaN/GaN MOS-HEMT for high-power rf applications.

The authors would like to thank H.-J. L. Gossmann for helpful discussions and GaN division of Cree Inc. (formerly Advanced Technology Materials, Inc.) for GaN growth.

[1] M. Asif Khan, X. Hu, G. Sumin, A. Lunev, J. Yang, R. Gaska, and M. S. Shur, IEEE Electron Device Lett. **21**, 63 (2000).
[2] M. Asif Khan, X. Hu, A. Tarakji, G. Simin, J. Yang, R. Gaska, and M. S. Shur, Appl. Phys. Lett. **77**, 1339 (2000).
[3] G. Simon, X. Hu, N. Ilinskaya, A. Kumar, A. Koudymov, J. Zhang, M. A. Khan, R. Gaska, and M. S. Shur, Electron. Lett. **36**, 2043 (2000).
[4] A. Koudymov, X. Hu, K. Simin, G. Simin, M. Ali, J. Yang, and M. Asif Khan, IEEE Electron Device Lett. **23**, 449 (2002).
[5] G. Simin, A. Koudymov, H. Fatima, J. Zhang, J. Yang, and M. Asif Khan, X. Hu, A. Tarakji, R. Gaska, and M. S. Shur, IEEE Electron Device Lett. **23**, 458 (2002).
[6] G. Simon, X. Hu, N. Ilinskaya, J. Zhang, A. Tarakji, A. Kumar, J. Yang, M. Asif Khan, R. Gaska, and M. S. Shur, IEEE Electron Device Lett. **22**, 53 (2001).
[7] X. Hu, A. Koudymov, G. Simon, J. Yang, M. Asif Khan, A. Tarakji, M. S. Shur, and R. Gaska, Appl. Phys. Lett. **79**, 2832 (2000).
[8] S. Ootomo, T. Hashizume, and H. Hasegawa, Phys. Status Solidi C **1**, 90 (2002).
[9] T. Hashizume, S. Ootomo, and H. Hasegawa, Appl. Phys. Lett. **83**, 2952 (2003).
[10] R. Mehandru, B. Luo, J. Kim, F. Ren, B. P. Gila, A. H. Onstine, C. R. Abernathy, S. J. Pearton, D. Gotthold, R. Birkhahn, B. Peres, R. Fitch, J. Gillespie, T. Jenkins, J. Sewell, D. Via, and A. Crespo, Appl. Phys. Lett. **82**, 2530 (2003).
[11] D. A. Buchanan, E. P. Gusev, E. Cartier, H. Okorn-Schmidt, K. Rim, M. A. Gribelyuk, A. Mocuta, A. Ajmera, M. Copel, S. Guha, N. Bojarczuk, A. Callegari, C. D'Emic, P. Kozlowski, K. Chan, R. J. Fleming, P. C. Jamison, J. Brown, and R. Arndt, in *Proceedings of the IEEE International Electron Devices Meeting* 2000, p. 223.
[12] G. D. Wilk, R. M. Wallace, and J. M. Anthony, J. Appl. Phys. **89**, 5243 (2001).
[13] P. D. Ye, G. D. Wilk, J. Kwo, B. Yang, H.-J. L. Gossmann, M. Frei, S. N. G. Chu, J. P. Mannaerts, M. Sergent, M. Hong, K. Ng, and J. Bude, IEEE Electron Device Lett. **24**, 209 (2003).
[14] P. D. Ye, G. D. Wilk, B. Yang, J. Kwo, H.-J. L. Gossmann, S. N. G. Chu, S. Nakahara, H.-J. L. Gossmann, J. P. Mannaerts, M. Sergent, M. Hong, K. Ng, and J. Bude, Appl. Phys. Lett. **83**, 180 (2003).
[15] P. D. Ye, G. D. Wilk, B. Yang, J. Kwo, H.-J. L. Gossmann, M. Sergent, M. Hong, K. K. Ng, and J. Bude, Appl. Phys. Lett. **84**, 434 (2004).
[16] S. C. Sun and J. D. Plummer, IEEE Trans. Electron Devices **ED-27**, 1497 (1980).
[17] J. S. T. Huang and G. W. Taylor, IEEE Trans. Electron Devices **ED-22**, 995 (1975).
[18] S. Takagi, A. Toriumi, M. Iwase, and H. Tango, IEEE Trans. Electron Devices **ED-41**, 2357 (1994).
[19] P. D. Ye, B. Yang, K. K. Ng, J. Bude, G. D. Wilk, S. Halder, and J. C. M. Hwang, in *Proceedings of the 2004 IEEE Lester Eastman Conference on High Performance Devices*, 2004, p. 24.

Downloaded 29 Oct 2006 to 128.46.221.220. Redistribution subject to AIP license or copyright, see http://apl.aip.org/apl/copyright.jsp